Accurate evaluation of the flow properties of molten chocolate: circumventing artefacts

Nathaniel J. Hendrik[a*], Flávio H. Marchesini[b], Davy Van de Walle[a], Koen Dewettinck[a]

[a] Ghent University, Faculty of Bioscience Engineering, Department of Food Technology, Food Safety and Health, Food Structure and Function Research Group, Coupure Links 653, 9000 Ghent, Belgium

[b] Ghent University, Faculty of Engineering and Architecture, Department of Materials, Textiles and Chemical Engineering, Technologiepark 130, 9052 Zwijnaarde, Belgium

*Corresponding author: e-mail: nathaniel.hendrik@ugent.be; Tel: +32 9 264 61 67

Abstract

Methods to characterize the flow behavior of molten chocolate have been set by International Confectionery Association (ICA) in 2000, however, there is no consensus on an accurate method and it is often followed by misinterpretation of the results. This issue is also influenced by flow phenomena generally recurring in yield-stress materials, such as transient effects, gap size effects, apparent wall slip and edge fracture. The state of the art in the field of rheology allow for more precise techniques to circumvent such rheometric artefacts. Nevertheless, a combined approach to accurately determine the flow properties of different types of molten chocolate targeting the prevention of all possible flow artefacts is still not found in the literature. In this paper, two technologically distinct molten dark chocolates are employed on different combinations of flow curve protocols, measuring geometries and viscosity functions to accurately determine their flow properties. Based on the evaluation, a wider shear rate range ($\dot{\gamma} = 0.01 – 100\ s^{-1}$) with sufficient measurement time per shear rate (> 120s) is recommended for an accurate flow curve protocol, combined with a roughened surface geometry with radii ratio < 1.10. Four-parameter mathematical models, such as the Windhab model or a modified Herschel-Bulkley model, have been proven to be more accurate in further acquiring important flow parameters, but special attention should be given to the physical meaning of some parameters. A comparison between experimental flow curve data, model-fitted data and steady-state data gained from a constant shear rate test confirmed the suitability of these recommendations for both chocolates. The proposed alternative method allows for accurate measurements at lower shear rates, which significantly improves the accuracy to obtain important parameters such as yield stress as well as detecting and preventing rheometric artefacts.

Keywords

Molten chocolate, yield-stress material, apparent wall slip, flow behavior, Casson model, Windhab model, modified Herschel-Bulkley model

Abbreviations

ICA: International Confectionery Association, IOCCC: International Office of Cocoa, Chocolate and Confectionery, MV: medium-viscosity chocolate, HV: high-viscosity chocolate

Introduction

The flow behavior of chocolate, a fat-based suspension consisting of sucrose and cocoa particles dispersed in a liquid cocoa butter phase, is important for many reasons. In their molten form, flow parameters provide valuable information on how to handle or transfer chocolate, including the matching flow rate for specific conventional applications, such as mold depositing, enrobing, dipping (Gray 2017), or more recent applications such as 3D printing (Mantihal et al. 2019). Furthermore, flow parameters play an important role during solidification of chocolate, as an incompatible flow behavior might cause poor final product quality, such as enrobed chocolate with "feet" (Wolf 2017). In addition, the flow behavior of chocolate is also important for the textural characteristics and, by extension, the sensorial perception, particularly the mouthfeel affecting the flavor release (Rodrigues et al. 2021).

The rheological properties of chocolate are affected by its production steps and its composition (Afoakwa et al. 2008; van der Vaart et al. 2013; Vásquez et al. 2019). The effect of refining is often characterized from the particle size distribution (PSD) and consequently the rheological properties of chocolate (Do et al. 2007; Glicerina et al. 2015; Rohm et al. 2018; Saputro et al. 2019). Impact on the flow properties from the composition of chocolate is evident, such as from its cocoa content (Fernandes et al. 2013), fat content (Do et al. 2007; Rodrigues et al. 2021), selection of (bulk) sweetener (Oba et al. 2017; Sokmen and Gunes 2006) and selection of dispersing agents (Schantz and Rohm 2005).

To properly characterize different chocolates and provide their application possibilities, International Chocolate Association (ICA) has developed a method involving flow curve test protocol, corresponding test geometries and mathematical model suggestions. The test protocol consists of recording the shear stress at increasing and, subsequently, decreasing shear rate, typically between 2 and 50 s^{-1}. This ICA 46 method suggests the usage of a viscometer or rheometer equipped with a temperature control unit and a coaxial measuring system. In addition, a proposed mathematical model fit to obtain the yield stress of the molten chocolate, an important flow parameter for a viscoplastic material, is also provided (ICA 2000).

Although such general guidance towards the measurement of the flow behavior of molten chocolate exists, the implementation of an accurate method and correct interpretation of the result remains an issue. In fact, an inaccurate rheological measurement method triggers flow phenomena and artefacts that might cause misleading interpretations (Barnes 1995; Coussot 2005; Keentok and Xue 1999; Manneville 2008; Marchesini et al. 2015; Mewis and Wagner 2009). It is therefore important to understand which artefacts that might occur during the flow behavior measurement of molten chocolate. Current advances in the field of rheology also make it possible to circumvent or minimize these problems.

Incompatible methodologies and rheological misinterpretation generally occur in suspensions, however, the most notable ones in molten chocolate are due to (i) insufficient measurement time to reach equilibrium, i.e. transient effects (Fischer 2015; Mezger

2014), (ii) inappropriate selection of shear rate range (Bolenz and Tischer 2013), (iii) interval selection for (thixotropy) interpretation (Barnes 1997; Coussot 2005; Mewis and Wagner 2009; Mezger 2014), (iv) gap size effect (Baker et al. 2006; Barnes 2000; Barnes and Nguyen 2001; Marchesini et al. 2015; Servais et al. 2003), (v) apparent wall slip (Barnes 1995; Marchesini et al. 2015), (vi) edge fracture (Coussot 2005; Keentok and Xue 1999), and (vii) selection of model fitting (Fischer 2015; Servais et al. 2003; Windhab 1995). All of these flow phenomena and artefacts are directly related to the setup of the flow measurement protocol, measuring geometry selection and mathematical model fitting selection.

Time-dependent effects become more significant for suspensions with high solid content and in the low shear rate range (Mezger 2014). These effects can introduce errors in the measurements of the flow curve, which must be built from steady-state data. Specifically, data points before the measurement equilibrate or while it is reaching a steady state could be inappropriately included as part of the flow curve (Fischer 2015). Such inclusion lead to uncertainty in the model fitting employed to determine flow curve parameters, such as yield stress. Current rheometers allow a more sensitive measurement at a lower shear rate range below 1 s^{-1} (Bolenz and Tischer 2013) in comparison to the proposed lowest shear rate in the ICA 46 method (ICA 2000), taking into account that the steady-state has been reached using appropriate geometry.

Increasing and decreasing shear rate in a flow curve measurement has been implemented ever since the predecessor of the current ICA 46 method for the sole purpose to have a qualitative evaluation of the thixotropy of molten chocolate (OICC 1973). Although it is convenient, it has been proven to be inaccurate while other accurate rheological tests to quantify thixotropy exist, such as three interval step test (Barnes 1997; Coussot 2005; Mewis and Wagner 2009; Mezger 2014). The further issue comes from selecting the interval for data interpretation, where recommendations vary between using the increasing interval (ICA 2000), descending interval (NCA/CMA 1988), or the average of both (OICC 1973). Taking into account descending interval is then contradicting the function of pre-shearing prior to the experimental interval, which is to standardize any shear history that occurs in the sample.

Apparent wall slip is a common flow phenomenon in yield-stress materials such as molten chocolate. Despite being the most popular standard geometry for flow behaviour measurement of chocolate, usage of smooth Couette concentric cylinder system are still susceptible to this phenomenon, especially at lower shear rates (Marchesini et al. 2015). This triggers research to overcome the problem by increasing the roughness of the geometrical surface, one of which is by using a vane geometry (Baker et al. 2006; Bergemann et al. 2018; NCA/CMA 1988). Though additional benefits of vane geometry to eliminate shear history exist, disproportionate surface roughness may also create secondary flows that further give complication to the measurement (Barnes and Nguyen 2001). Furthermore, just like Couette concentric cylinder, the gap size of vane geometry is limited and often this gap size effect is overlooked without any correction (Servais et al. 2003). This triggers several other researchers to start experimenting with (roughened-surface) parallel plates (Baldino et al. 2010; Vásquez et al. 2019), although the risk of flow instability, due to the surface tension between the plates might cause another phenomenon, namely edge fracture (Coussot 2005; Keentok and Xue 1999).

One of the biggest issues in the rheology of molten chocolate is the consensus on appropriate mathematical model fitting, as the importance to obtain yield stress value is of high priority. Most users of ICA method choose the model fit of Casson, which is the model proposed by the previous version of ICA 46 (OICC 1973), created by the predecessor of ICA, the International Office of Cocoa, Chocolate and Confectionery (IOCCC). However, the current ICA 46 method suggests the usage of the four-parameter Windhab model instead (ICA 2000; Windhab 1995). Regardless of its popularity, several researchers found the Casson model to be inaccurate at lower shear rate ranges and find solution by using the Carreau model (Fernandes et al. 2013; Taylor et al. 2009; Vásquez et al. 2019), power-law model (Glicerina et al. 2016; Vásquez et al. 2019), or Herschel-Bulkley model (Chevalley 1994; Talansier et al. 2019).

Regardless of the numerous issues in the methodology, approaches to solve this issue has been plentiful for yield-stress material, including molten chocolate. The importance of a longer measurement time has been apprehended to achieve accurate results at a lower shear rate range, although steady-state at the selected shear rate is not evident (Bolenz and Tischer 2013; Talansier et al. 2019). Correct usage of measuring geometries, appropriate gap size and importance of roughened surface to suppress apparent wall slip, protrusion flow and edge fracture is abundant for suspensions with hard particles (de Souza Mendes et al. 2014; Marchesini et al. 2015), though it is still lacking for molten chocolate. Comparison between mathematical models and their weaknesses and strengths has been reviewed for food suspensions (Fischer 2015; Glicerina et al. 2016).

However, approaches to detect and prevent flow artefacts in molten chocolate are often (i) selective to solve a specific issue, (ii) directed toward a specific formulation, process and type of molten chocolate and (iii) neglecting the interrelation of available methodologies. The objective of this paper is to provide an accurate determination of the flow properties of molten chocolate by combining appropriate setup and usage of flow measurement protocol, geometry and model fitting. Two rheologically distinct molten chocolates designed for different applications were employed on an extensive combination of flow behaviour measurement methodologies. Hereby, an overview of possible flow phenomena and artefacts in molten chocolate was evaluated. Finally, a suitable combination of flow behaviour measurement is proposed and validated with experimental and steady-state data.

Materials and methods

Samples preparation

Two different dark chocolates (Belcolade, Erembodegem, Belgium) showing a distinct technological functionality were used: medium-viscosity chocolate (MV) and high-viscosity chocolate (HV). MV consists of 55% cocoa and is used for common chocolate applications, such as molded bars. HV consists of 50% cocoa and is used for bake-stable applications, such as heat-resistant inclusions.

MV and HV were originally in the form of chocolate callets. Prior to rheometric measurements, they were kept in a sealed plastic container and placed in a thermostatic chamber Terma 2S (LED techno, Heusden-Zolder, Belgium) at 52°C ± 0.2°C. MV was kept for a minimum of 2 hours and HV was kept for a minimum of 3 hours to ensure liquid sampling.

Composition & particle size distribution analysis

Moisture content (% w/w) of MV and HV was calculated on the basis of dry matter following the gravimetrical method using oven drying as described in the official method of Association of Analytical Chemists (AOAC) 931.04 (AOAC 1990b). The total fat content (% w/w) of MV and HV was measured following the extraction method AOAC 963.15 (AOAC 1990a) with some modifications. 5g of sample was weighed and acid digested. Soxhlet extraction with extra pure petroleum ether (Thermo Fischer Scientific, Loughborough, UK) was performed subsequently. The extracted lipids were then measured gravimetrically. Both chemical analyses were performed in triplicate.

The free fat content (% w/w) of the chocolates was determined following the method of (Saputro et al. 2019) with some modifications. 12 g of extra pure petroleum ether (Thermo Fischer Scientific, Loughborough, UK) was added to 5 g of molten chocolate and was then mixed using a vortex. The mixture was centrifuged using Sigma Centrifuge 4K15 (Sigma Laborzentrifugen GmbH, Germany) for 10 min at 9000 rpm. The supernatant was then separated by pouring it into a bulb flask. The same procedure was applied 2 more times to the precipitate. Subsequently, the total supernatant was put in a vacuum rotary evaporator for 10 min at 60 °C to evaporate the solvent. The bulb flask was put in the oven at 105 °C for 2 h to further evaporate remaining solvent before the free fat was gravimetrically measured. The analysis was performed in triplicate.

The particle size distribution (PSD) of MV and HV was analyzed using Malvern Mastersizer S Long Bench (Malvern Instruments Ltd., Worcestershire, UK) equipped with a 300 RF lens to measure particles in the range of 0.05 – 900 µm. Approximately 0.5g of chocolate was diluted in 10 ml of isopropanol and then heated in an oven at 55°C for at least 1h. Prior to the measurement, the chocolate suspension was subjected to ultrasound waves at 80 Hz for 15 mins to break loose agglomerates. Smallest particle size (d_{10}), mean particle size (d_{50}), largest particle size (d_{90}), mean particle diameter ($d_{4,3}$), Sauter mean diameter ($d_{3,2}$) and arithmetic mean diameter ($d_{1,0}$) were obtained as the PSD parameters. PSD was performed in triplicate with three dependent repetitions for each replicate.

Rheometrical methods

All rheological measurements were performed using a stress-controlled rheometer MCR 302 (Anton Paar GmbH, Graz, Austria) at a constant temperature of 40.0°C ± 0.2°C controlled with a Peltier system connected to a Paar VT2 refrigerated circulator (Julabo, Seelbach, Germany).

<u>Flow curve measurement protocols</u>

Flow curve measurements were performed in the following order: pre-shearing, increasing shear rate interval, constant shear rate and decreasing shear rate interval following the standard ICA 46 protocol. Two standard ICA 46 protocols (continuous and stepwise) and a new protocol were applied (Table 1). All measurements were done in triplicate and the averages are reported. When artefacts, such as apparent wall slip and edge fracture phenomenon are prevented, the maximum experimental error reached 12.8%.

The standard ICA 46 protocol suggests that measurements can be performed continuously or stepwise at specific shear rates. Opting for continuous measurement in the MCR 302 rheometer automatically selects the shear rate over the total measuring time evenly (Table 1). Duration of each measurement at each shear rate was set to 1 s as the default recommended for continuous measurement by MCR 302.

A new proposal stepwise (NPs) protocol was set up to offer a longer measurement time at each shear rate and a broader shear rate range to ensure more accurate data for model fitting purposes. The shear rates were selected to ease the comparison of values at the same shear rate with the ICA 46 stepwise (ICs) flow curve protocols.

<u>Flow curve measuring systems</u>

The rheological experiments were performed using five measuring systems (Table 2). The smooth concentric cylinders and smooth vane-in-cup measuring systems shared the same measuring cup of 14.47 mm radius. Measuring bob of concentric cylinder had a radius of 13.33 mm and the vane radius was 12.00 mm, making each having a fixed measuring gap for both cylindrical measuring systems, as stated in Table 2. While the measuring gaps for all 3 parallel-plate geometries are flexible, they were set to 1.00 mm.

<u>Flow curve model fitting</u>

The increasing shear rate data of the flow curve test were fitted with two mathematical models. The former IOCCC method (Aeschlimann and Beckett 2000) suggests the usage of the Casson model (Eq. 1). Conversely, the most recent ICA method (ICA 2000) suggests the usage of the Windhab model (Eq. 2). Both models are as follows:

$$\sqrt{\tau} = \sqrt{\tau_C} + \sqrt{\eta_C \cdot \dot{\gamma}} \quad (1)$$

$$\tau = \tau_0 + (\tau_1 - \tau_0) \cdot [1 - exp\,(-\dot{\gamma}/\dot{\gamma}^*)] + \eta_\infty \cdot \dot{\gamma} \quad (2)$$

where τ_C and η_C are respectively the Casson yield stress (Pa) and Casson plastic viscosity (Pa.s), whereas τ_0, τ_1, $\dot{\gamma}^*$, and η_∞ are respectively the yield point or static yield stress (Pa), the shear stress that leads to the "maximum shear-induced structural change" or dynamic yield stress (Pa), the characteristic shear rate (s^{-1}) as an approximation parameter where the shear-induced structure has already been built up and the constant high shear viscosity or infinite viscosity (Pa.s) (ICA 2000; Mezger 2014). The fit quality of each of the model was evaluated using determination coefficient (R^2).

In addition to mathematical models proposed by ICA, a modified Herschel-Bulkley model as discussed by de Souza Mendes (2011) was employed as another 4-parameter model proposal:

$$\tau = \tau_0 + k \cdot \dot{\gamma}^n + \eta_\infty \cdot \dot{\gamma} \quad (3)$$

where τ_0, k, n and η_∞ are respectively the yield stress (Pa), the consistency index, the power-law index and the viscosity at infinite shear rate (Pa.s).

Non-linear curve fitting of experimental data with the mathematical model of Casson, Windhab and modified Herschel-Bulkley were performed using Kaleidagraph 4.0 (Synergy, Pennsylvania, USA). Statistical analysis was performed with SPSS statistics 28 (SPSS Inc., Illinois, USA). Each of the flow parameters from Casson, Windhab and modified Herschel-Bulkley model from different chocolate, measurement protocol and measuring systems were subjected to a three-factor Analysis of Variance (ANOVA) with a 5% significance level. Assumptions of normality and equality of variance were tested prior to the analysis using Shapiro-Wilk test and Modified Levene's test, respectively. When three-way interactions exist, a post-hoc Tukey's test was used to further examine between different levels of each factor. When only two-way interactions exist, factors without significant difference were used to split the data and a two-way ANOVA was performed with a 5% significance level. When assumptions were fulfilled, a post-hoc Tukey's test was used to investigate different levels of predictors.

<u>Constant shear rate tests</u>

Constant shear rate tests of MV and HV were performed using 50-mm sandblasted parallel plates at shear rates of interest, which was also used in the flow curve test ICs and NPs (Table 1). The measurement time changed with every decade of shear rate from 7200s for the lowest shear rate to 100s for the higher shear rate. The measurements were taken logarithmically from every 0.1 to every 100s. All constant shear rate tests were done in triplicate and reported as averages. When artefacts, such as edge fractures were disregarded, the maximum experimental error reached 13.0%.

Results and discussion

Methodologies to measure the flow behavior of molten chocolate are discussed in this section. First, the effect of formulation and prior chocolate processing on the flow behaviour of two technologically distinct chocolate are evaluated from the compositional and PSD analysis. Then, flow phenomena and artefacts that occur due to different combinations of flow curve protocols, measuring geometry and model fit were showcased and were utilized as the basis to recommend a methodology. Finally, results from the proposed recommendation were validated by comparing experimental, model fit and steady-state results.

Composition & PSD analysis

The presence of moisture is generally influenced by the refining and conching process, in which sucrose particles might absorb humidity during the process. Moisture should be avoided and regulated to a level below 1% since it also increases the viscosity of molten chocolate (Afoakwa et al. 2008) . HV showed a significantly higher moisture content in comparison to MV with a value of 1.01 ± 0.04% (Table 3). This might already explain the technological purpose of HV where viscosity is purposely increased through the increase of moisture content. This level is reportedly high in comparison to chocolate for standard applications (Saputro et al. 2019; Sokmen and Gunes 2006), which is in the agreement for MV with 0.65 ± 0.03%.

Total fat content and free fat content (Table 3) also confirmed the distinction of formulation between MV and HV. HV has a significantly lower fat content in comparison to MV, thus, HV has a significantly higher solid fraction. Higher solid fractions reportedly contribute to higher viscosity values (Do et al. 2007; Rodrigues et al. 2021). The result of total free fat content is also in line with total fat content, where it is describing the free cocoa butter that is unbound with- or intrapped within cocoa solid particles. Cocoa butter is generally added to reduce yield stress and viscosity of molten chocolate (van der Vaart et al. 2013). Higher free fat content in MV might indicate extra cocoa butter added during the chocolate manufacturing process.

The comparison of PSD parameters between MV and HV is shown in Table 3, where variations between both chocolates are observed on d_{50}, d_{90} and $d_{4,3}$. The largest particle size in PSD has been correlated with the fineness that can be perceived during consumption but also affects the flow parameter of the chocolate. Lower d_{90} has reportedly resulted in a higher value of viscosity and yield stress (van der Vaart et al. 2013). This might be an indication of different refining processes or protocols, as the largest particle size of chocolate is normally pre-determined during the refining process (Glicerina et al. 2015; Rohm et al. 2018). However, it has been reported that PSD during refining can be affected by the total fat content during formulation (Afoakwa et al. 2008). Nevertheless, compositional and PSD analysis in Table 3 demonstrated a clear distinction between MV and HV that resulted in different flow behaviour between both chocolates.

Flow phenomena & artefacts

Transient effects and shear banding

To evaluate and select sufficient measurement time to reach the equilibrium state for the newly proposed flow curve protocol, a constant shear rate test was performed. The evolution from transient viscosity into steady-state viscosity is shown in Fig. 1, where the time-dependent flow behavior of MV and HV was observed at each shear rate point that is used in both ICA and the newly proposed protocol. Mezger (2014) emphasized the importance of sufficient measurement time to avoid transient effects that may occur at lower shear rates for time-dependent flow behavior. Measurement time also became one important factor of correction of the IOCCC (2000) method into ICA 46 (ICA 2000), where the measurement time of different laboratories had a significant effect on Casson flow parameters using the same chocolate (Aeschlimann and Beckett 2000). The steady-state tests in our research were performed using only sandblasted parallel plate 50 mm and it is clear that for MV (Fig. 1a) at the range of ICA protocol (2-50 s^{-1}), steady-state viscosity has been reached within 16 s, the approximate measurement time at each shear rate. However, at lower shear rates, such as from 0.1-1 s^{-1}, transient viscosity is still observed reaching an equilibrium at 16 s. Hence, 120 s measurement time at each shear rate using the newly proposed protocol is proposed to ensure that the flow curve records steady-state viscosity.

In Fig. 1a, it can also be noticed within 0.01-0.09 s^{-1} the equilibrium seemed not to be attained even after almost 10000s of measurement time. Although the plateau explains the discrepancy of higher viscosity value at such shear rate in the new proposal stepwise protocol, the constant shear rate test result also accounts for possible need of a longer time frame to reach steady-state. This issue can occur especially on a dense suspension with a specific matrix volume fraction (Ianni et al. 2008; Manneville 2008). This might explain why HV (Fig. 1b), which has higher solid content, reached equilibrium whereas MV (Fig. 1a) still has not reached equilibrium even after 7200 s. This also stresses the importance of a constant shear rate test to confirm measurement time and shear rate range required in the flow curve protocol, especially when a lower shear rate is employed in the flow curve protocol.

The importance of measurement time in the flow curve protocol can also be seen by comparing the increasing shear rate interval of ICA stepwise and continuous protocol in Fig. 1. Contrary to the claim of ICA (2000), usage of both protocols generated a significantly different result. Apparent viscosity values within 2 – 30 s^{-1} of ICA continuous protocol were in agreement with steady-state values (Fig. 1), in which they are generally higher than the values obtained from ICA stepwise protocol. Yield-stress material requires time to reach the equilibrium state where all of the suspended particles are well oriented hence showing steady-state viscosity (Mezger et al., 2014). The continuous protocol in ICA continuous protocol only allows 1 s per measuring point. This is not enough for the sample to equilibrate at the lower shear rates during the upward interval, regardless of the geometry used. As a result, different magnitudes of hysteresis loop are obtained, therefore leading to inaccurate flow parameters, especially at low shear rates. It is then recommended to always perform a stepwise flow curve test over a continuous test, taking into account enough time to equilibrate prior measurement at each selected shear rate.

Selecting the appropriate shear rate range

Aside from characterizing molten chocolate flow behavior at rest, measurement at a lower shear rate is also significant to obtain accurate yield stress values. Fig. 2 compares the shear stress curve between the ICA stepwise protocol and the new proposal protocol using a concentric cylinder system. The newly proposed protocol allows measurement of shear stress at a shear rate value down to 0.01 s^{-1}. This will already benefit model fitting in comparison to the usage of ICA protocol, where the lowest measured shear rate is at 2 s^{-1}. Determination of yield stress is done by extrapolating the flow curve towards $\dot{\gamma}$ = 0 s^{-1} (Mezger 2014), hence obtaining more data on shear stress during the flow test at low shear rates will improve the accuracy.

While the results between the two protocols seemed to be in accordance with the shear rate range suggested by the ICA protocol (2 - 50 s^{-1}), values outside of such shear rate range are significantly different, especially at lower shear rates. ICA 46 method allows usage of a viscometer where irreproducibility of results might still be high due to its sensitivity (Fischer 2015; Mezger 2014), however, current flow measurements have inclined toward controlled shear stress or controlled shear rate rheometer. Achieving reproducible results at lower shear rates, regardless of the measuring geometry, has been proven possible for molten chocolate (Bolenz and Tischer 2013; Fernandes et al. 2013; Talansier et al. 2019; Vásquez et al. 2019), although it is worth to note that the steady-state should not be violated.

Several flow phenomena can be noticed in the newly proposed protocol in Fig. 2 that could not be observed in the shorter ICs protocol. This includes the distinct hysteresis loop areas and the kinks occurring at shear rates below 0.1 s^{-1} in MV or below 0.2 s^{-1} in HV. Hence, exploring wider shear rate ranges provides more information on the flow behavior, including phenomena that could be geometry-dependent or subject to inaccuracy in the measurement.

Selecting measurement interval for (thixotropy) interpretation

The degree of thixotropy can be qualitatively described from a hysteresis loop, that is when a flow curve from a consecutive increasing and decreasing shear rate ramp do not coincide (Afoakwa et al. 2009; Servais et al. 2003). The difference of values between two different intervals is reflected in the viscosity curve comparison between ICA stepwise and continuous protocol in Fig. 3. Although the effect of insufficient measurement time of continuous protocol (1s per shear rate) is observed here, the hysteresis loop was always substantially bigger in the continuous protocol, while the magnitude seems to be dependent on the type of chocolate. No hysteresis loop was observed in the flow curve of the stepwise protocol of MV, while it is evident at a lower shear rate, such as at 5 s^{-1}, that hysteresis occurs in the continuous protocol in Fig. 3a. Nevertheless, hysteresis loop also exists in the flow curve of the newly proposed protocol of MV in Fig. 2 indicating the shear history dependency of this method to interpret thixotropy.

Calculating the difference between stress during continuous increase and decrease in a flow test for materials with yield stress was one of the strategies utilized to evaluate the thixotropy of suspensions (Green and Weltmann 1943) and was later employed by the

ICA standard (Servais et al. 2003). However, the result of the hysteresis loop with this method is dependent on the shear history and the shear rate value, hence also dependent on the selection of rheological protocol and geometry, making it inaccurate to measure true material properties (Barnes 1997; Mewis and Wagner 2009). This method is a mere empirical estimation, which is for quality control purposes. Nowadays, more accurate tests, such as the three-interval test, are used to investigate thixotropic behavior (Coussot 2005; Mezger 2014). Taking into account of the shear history effect, further on in this paper, only increasing shear rate interval values will be shown in flow curves.

Effect of gap size when selecting geometry

Fig. 4a shows the shear stress curve of MV measured with ICs protocol with different geometries. While all the shear stress values of the sample measured with parallel plate seem to be in the same range, the sample measured with cylindrical systems, particularly smooth vane-in-cup, deviates exceedingly. Such deviation is expected in this experiment, as the gap between the inner and outer cylinders of these cylindrical measuring systems are not the same and incompatible as the gap employed in the parallel plate geometries. Baker et al. (2006) observed the effect of measurement gap size in vane-in-cup as the vane height and diameter ratio variation affected the value of yield stress obtained. A correction calculation is needed as an end effect is expected when the radius ratio of radii between inner and outer circumference exceeds 1.10 (Barnes 2000; Meeten and Sherwood 1992; Servais et al. 2003), which might be the reason for the deviation in the result of our vane geometry since the ratio of radii is 1.21.

Vane geometry was initially employed to solve the apparent slip problem that normally occurs in smooth Couette cylinders because of the presence of continuous fluid at the wall (Dzuy and Boger 1983; Yeow et al. 2000). Therefore, the usage of vane has been implemented as an alternative to measure flow behavior of chocolate (Bergemann et al. 2018; Servais et al. 2003). In addition, it also serves as a validation technique to obtain yield stress by extrapolating data from a flow curve obtained with the Couette geometry (Baker et al. 2006; Wilson et al. 1993). It became a method that is widely employed in the United States (NCA/CMA 1988), set by Chocolate Manufacturers Association (CMA). Although the usage of vane is claimed to be accurate to obtain true yield stress value, it requires correction calculation to obtain apparent viscosity values (Servais et al. 2003). Moreover, the vane-in-cup measuring system can present secondary flows between the blades of the vane at higher shear rates as well as apparent wall slip at the outer smooth cylinder wall (Barnes and Nguyen 2001). This is a possible explanation for the gradual decline of the shear stress value at a lower shear rate from usage of vane geometry, which is consistently independent from protocol and type of chocolate (Fig.3a – Fig.3d). Hence, it can be concluded that in our experiment, vane-in-cup is not suitable to obtain accurate flow curve values. Care should be taken when vane geometry is employed due to compatibility and flexibility of gap size and the possibility of apparent wall slip at the outer smooth cylinder.

Apparent wall slip

Fig. 4c and 4d show the shear stress curve of MV and HV, respectively, measured using the newly proposed protocol with different geometries. In both figures, irregular non-linear kinks occur at shear rates below 0.1 s^{-1} for MV and around 1 s^{-1} for HV, more specifically for measurements using smooth surfaces (parallel plates and concentric cylinders). These specific bends in the flow curve at a lower shear rate were possibly caused by the formation of a thin oil layer acting as lubricant, facilitating flow and, hence, decreasing the apparent viscosity (Barnes 1995; Marchesini et al. 2015; Yoshimura and Prud Homme 1988); a phenomenon that is called as apparent wall slip.

Although it is common to observe apparent wall slip phenomenon in non-Newtonian suspensions with hard particles, this phenomenon is often not fully comprehended and misinterpreted in chocolate rheology. This misconception could be due to the fact that the lower limit of the shear rate in the flow curve test in ICA 46 (2 s^{-1}) cannot detect apparent wall slip, which manifests at shear rates lower than range employed in standard viscosity measurements of chocolate (ICA 2000). When apparent wall slip occurs, it is commonly mistakenly interpreted as flow characteristics of the chocolate due to its microstructure (Fernandes et al. 2013; Schantz and Rohm 2005; Taylor et al. 2009; Vásquez et al. 2019). This triggers several researchers to have an approach to solve this apparent wall slip issue in chocolate (Bergemann et al. 2018; Servais et al. 2003; Talansier et al. 2019).

The apparent wall slip phenomenon has been an interesting issue in thixotropic yield-stress materials. Apparent wall slip issues occurring in hard particle suspensions can be solved in two ways: (i) quantification and correction of the apparent wall slip by comparing results obtained at different gap sizes (Yoshimura and Prud Homme 1988) and (ii) modification of the nature of the wall of the measuring system from smooth to rough (Buscall et al. 1993). Strategy (i) requires a lot of measurements at different gaps and a lot of mathematical processing to obtain slip velocity, which can then be calculated to correct the apparent wall slip below the yield stress (Barnes, 1995). Whereas strategy (ii) is more straightforward; although changing the surface roughness of the measuring system must be properly done by determining the wall roughness with the size of the largest particles in the matrix. Incompatible lower roughness will cause inefficient apparent wall slip prevention and higher roughness, such as usage of vane-in-cup geometry, may trigger secondary flows (Buscall et al. 1993; Mansard and Colin 2012; Ovarlez et al. 2011).

While the majority of the chocolate research works still follows the most currently accepted standard of ICA 46, only few studies focused on solving the apparent wall slip problem. Talansier et al. (2019) have adapted the quantification method to obtain slip velocity equations and improved the approach of Yoshimura and Prud Homme (1988) by extending reciprocal gap range and ensuring all viscosity data are in steady-state. Servais et al. (2003) suggested the use of vane geometry only to find the correct yield stress value, as the apparent viscosity value still needs to be corrected by infinite gap correction. Bergemann et al. (2018) made a custom geometry by using a customized vane in a glass beaker with a coating of sub-millimeter glass beads.

The deviating shear stress at lower shear rate (Fig. 4c and Fig. 4d) did not occur when roughened geometries are used, indicating that both sandblasted parallel plates suppressed apparent wall slip at lower shear rate. While this strategy to suppress apparent wall slip has been recommended for yield-stress material in general (Barnes 1995; Coussot 2005; de Souza Mendes et al. 2014; Marchesini et al. 2015), usage for molten chocolate is still lacking with only Baldino et al. (2010) reportedly using serrated parallel plate yet for an oscillatory test, not for a rotational flow curve test. Both sandblasted parallel plate with 50- and 25-mm diameter, having dimensions (Table. 2) larger than the size of particles in both MV and HV, worked well in our experiment to measure flow parameters at lower shear rate, as shown in Fig. 4c and Fig. 4d. Our finding confirms the benefit of the correct roughened surface geometry to avoid apparent wall slip on molten chocolate flow behavior measurement.

Edge fracture

The limitation of parallel plate geometry is showcased in Fig. 4b and Fig. 4d, where the shear stress curve of HV was measured with ICA stepwise protocol and newly proposed stepwise protocol in combination with different geometries. It is clear that the shear stress value decreases above 45-50 s^{-1} in samples measured with parallel plate geometry, defying the shear-thinning characteristics of molten chocolate as a non-Newtonian material. This instability, because of centrifugal forces that are higher than the surface tension between the parallel plates, is described as edge fracture, characterized by indentation on the free surface of the material at a critical shear rate (Barnes et al. 1975; Keentok and Xue 1999). Edge fracture also reflects on steady-state measurement, wherein a matrix with a higher volume fraction such as HV in Fig. 1b, equilibrium can be reached within a shorter period compared to the matrix with lower volume fraction such as MV. The steady-state test result at shear rate range 45-90 s^{-1} shows correlation with such phenomenon, which confirms the deviation in newly proposed protocol. The edge fracture in the highly viscous HV occurs as the parallel plate fails to hold the sample at a higher shear rate, causing sample to spill and a decrease in the shear stress. Herewith, to avoid edge fracture at a higher shear rate, usage of concentric cylinders is more recommended as samples are retained in the cup at a higher shear rate. It should be noted that too high shear rates should not be employed in rotational rheometry as this condition is not considered in the rheometer theory.

Selection of model fitting

It is predominantly evident that selection of protocol and geometry has an impact on different fitting parameters, as showcased in Table 4. Yield stress, an important flow parameter for molten chocolate has been shown significantly different regardless of the type of chocolate or model used. This significance strongly indicates the importance of lower shear rate value in obtaining accurate yield stress that comes from extrapolation towards $\dot{\gamma}$ = 0 s^{-1} (Mezger 2014). Artefacts occurring while investigating the importance of measuring protocol and measuring system, such as apparent wall slip and edge fracture, were disregarded prior to mathematical model fitting. This is so because it would not make sense to employ unreliable data for model fitting. This stresses the importance of an accurate protocol and geometry selection prior to measurement and model fitting.

Fig. 5 shows combinations of shear stress curves on MV and HV produced with the ICA-recommended method and a stepwise new proposal protocol with a wider shear rate range and sandblasted parallel plate, all including the fit to Casson, Windhab and modified Herschel-Bulkley model. Fig. 5a shows that with ICA 46 suggested protocol and geometry, the Casson mathematical model seemed to fit relatively well the flow curve of MV, supported by the determination coefficient value at 0.98 in Table 4. This could be the reason why ICA 46 with the Casson model is the most popular and widely employed, along with the fact that it consists of only 2 parameters, making the interpretation quite simple. However, it can be observed in Fig. 5a that it is not the same case for HV. Deviation from the direct measurement values is significantly different from the fit at $\dot{\gamma}$ = 2 s^{-1}. The limitation of Casson was also confirmed when a wider shear rate range is employed (Fig. 5c and Fig. 5d). Since it consists of only 2 parameters, Casson's mathematical model is not suitable to describe the non-linear flow behaviour that molten chocolate has, especially at a lower shear rate range. This has been discussed by Servais et al. (2003) as the limitation of using Casson's model and why Windhab's model is being introduced.

Windhab's model is based on 4 parameters and hence provides more insight into the flow curve, as stated in Table 4. Windhab introduce τ_0 and τ_1, which are the minimum stress required to initiate flow and the minimum stress required to maintain a maximum shear-induced structural change, respectively (ICA 2000). Windhab's model in all combinations (Fig. 5) fitted the experimental data well, except on HV when ICA stepwise protocol is employed along with sandblasted parallel plate in Fig. 5b with R^2 = 0.996. It can also be noted that it gives a different (static) yield stress value (τ_0) compared to Casson's yield stress (τ_C) . This elucidates the limitation of Casson’s model in which Windhab’s model is able to link the parameters to true physical behaviour occurring in the microstructure, by separating stress needed to initiate and maintain flow (Aeschlimann and Beckett 2000; Servais et al. 2003). It should be noted that the existence of two distinct yield stresses in the Windhab’s model implies a non-monotonic flow curve. However, this is not observed in the experimental data obtained for the two different dark chocolates, which can indicate a limitation of this model in accurately describing the observed physical behavior.

A modified Herschel-Bulkley model, which also consists of 4 parameters, was employed to show different model-fitting approaches and how the selected parameter will affect the quality of the fit. Result from determination coefficient for this modified Herschel-Bulkley model suggests that it has the best quality of fit on all combinations of protocol & geometry (R^2 = 0.999) among other selected model (Table 4). Moreover, the model was able to differentiate yield-stress produced through different methodologies, indicating the accuracy of the model to obtain values at the selected parameter. Like the simple Herschel-Bulkley model, this modified model utilizes consistency index, *k*, and power-law index, *n*, as the material parameter, while taking into account that only one true yield stress exists in the material. At the same time, this model utilize the steady-state experimental information, that is when after some time, the structuring in microstructure does not change anymore, reflected in the viscosity reaching shear rate at infinity, η_∞ (de Souza Mendes 2011). This is also confirmed with the steady-state data in Fig. 5, which might explain the improved accuracy using this model.

Validation of the newly proposed protocol

Based on the evaluation of flow phenomena and artefacts involving selection of methodologies in previous section, it is recommended to perform flow curve test with wider shear rate range while having sufficient measuring time per shear rate, as reflected in the new proposal stepwise protocol, combined with a roughened surface geometry and employing a mathematical model fit that takes into account thixotropic behavior. Comparison between shear stress from constant shear rate tests at 120s and the new proposal protocol performed with sandblasted parallel plates fitted with modified Herschel-Bulkley model is shown in Fig. 6. The steady-state test result follows the trend and is comparable to both flow curve results and modified Herschel-Bulkley's model fit for both chocolates, validating that the combination of newly proposed stepwise flow curve protocol and roughened surface geometry can be a good approach to obtain accurate flow curve parameters for dark chocolates.

Values of shear stress from the flow curve at other shear rates are mostly lower than values of shear stress obtained from the constant shear rate test. Molten dark chocolate as a dense suspension exhibit time-dependent flow properties where time is required for the material either to reach equilibrium state when particles undergo shear-induced deagglomeration and orientation, or a reversible mechanism (Windhab 2006). This thixotropic behavior also causes the effect of shear history toward the flow behavior of chocolate. Unlike series of constant shear rate tests, the flow curve test is more efficient since it gives information on wide shear rate range in one test. However, the trade-off is that thixotropic materials have historical time-dependent shear effects (Barnes 1997), as in the case at lower shear rates in Fig. 6. Approaches to investigate the effect of shear history comprise series of creep tests (García et al. 2015) or modelling through numerical calculations (Rathee et al. 2021), however, it is rather more time-consuming in comparison to performing a flow curve test. Hence, series of constant shear rate tests here was performed to validate flow curve protocol.

Conclusions

The importance and interrelationship between the appropriate rheometrical methodologies, from measurement protocol, geometry and model-fitting has been showcased in this paper by comparing two extremely technologically and rheologically distinct chocolates. The wider shear rate range in the measurement protocol ensures a better observation of flow phenomenon and artefacts that could be misinterpreted and avoided to reduce inaccuracy, such as apparent wall slip and edge fracture. Utilization of roughened surface parallel plate has been proven to prevent apparent wall slip that commonly occurs at a low shear rate using smooth concentric cylinders. Through this proper use of measurement protocol & geometries, the accuracy of model fitting was improved, with both the 4-parameter model of Windhab and modified Herschel-Bulkley proven to produce more reproducible and accurate flow parameters in comparison to the more popular 2-parameter model of Casson.

The steady-state flow of both chocolates was also investigated and the results are in line with the result of the flow curve, validating the accuracy of the proposed protocol, geometry and model fitting. In addition, by examining the steady-state, a better understanding of flow phenomena can be utilized to improve methodology and might be a useful tool in further characterizing the flow behavior of different types of molten chocolate in the future.

List of tables

Table 1. Flow curve protocols

Flow curve protocols	Pre-shear	Shear rate increasing	Shear rate constant	Shear rate decreasing	Shear rates (s^{-1})	Measurement time per shear rate (s)
ICA 46 continuous	5 s^{-1} for 300s	2-50 s^{-1} for 180s	50 s^{-1} for 60s	50-2 s^{-1} for 180s	2, 6.8, 11.6, 16.4, 21.2, 26, 30.8, 35.6, 40.4, 45.2, 50	1
ICA 46 stepwise	5 s^{-1} for 300s	2-50 s^{-1} for 180s	50 s^{-1} for 60s	50-2 s^{-1} for 180s	2, 5, 10, 15, 20, 25, 30, 35, 40, 45, 50	16.36
New proposal stepwise	5 s^{-1} for 300s	0.01-90 s^{-1} for 2400s	90 s^{-1} for 60s	90-0.01 s^{-1} for 2400s	0.01, 0.02, 0.05, 0.07, 0.09, 0.1, 0.2, 0.5, 0.7, 0.9, 1, 2, 5, 7, 9, 10, 20, 50, 70, 90	120

Table 2. Rheological measuring system and the geometrical data

Geometry	Inner diameter (mm)	Measuring gap (mm)
Smooth concentric cylinder	26.65	1.14
Smooth vane-in-cup	24.00	2.47
Smooth parallel plate	50.00	1.00
Sandblasted parallel plate	50.00	1.00
Sandblasted parallel plate	25.00	1.00

Table 3. Composition and particle size distribution of MV and HV

Composition	MV	HV
Moisture content (% w/w)	0.65 ± 0.03^a	1.01 ± 0.04^b
Total fat content (% w/w)	35.87 ± 0.09^a	27.98 ± 0.06^b
Total free fat content (% w/w)	34.36 ± 1.56^a	26.84 ± 1.24^b
d_{10} (μm)	1.13 ± 0.07^a	1.07 ± 0.11^a
d_{50} (μm)	6.34 ± 0.19^a	5.84 ± 0.23^b
d_{90} (μm)	22.58 ± 0.77^a	20.82 ± 0.59^b
$d_{4,3}$ (μm)	9.52 ± 0.27^a	8.82 ± 0.29^b
$d_{3,2}$ (μm)	2.40 ± 0.14^a	2.24 ± 0.19^a
$d_{1,0}$ (μm)	0.18 ± 0.03^a	0.16 ± 0.01^a

Table 4. Summary of flow parameters obtained by using Casson, Windhab and modified Herschel-Bulkley model from the two chocolates using the stepwise protocol of standard ICA 46 and new proposal protocol with two selected geometry

	Medium-viscosity chocolate (MV)				**High-viscosity chocolate (HV)**			
	ICA stepwise		New proposal stepwise		ICA stepwise		New proposal stepwise	
	Smooth conc. cylinder 27 mm	Sandblasted parallel plate 50mm	Smooth conc. cylinder 27 mm	Sandblasted parallel plate 50mm	Smooth conc. cylinder 27 mm	Sandblasted parallel plate 50mm	Smooth conc. cylinder 27 mm	Sandblasted parallel plate 50 mm
Corresponding graph	***Fig. 5a***	***Fig. 5b***	***Fig. 5c***	***Fig. 5d***	***Fig. 5a***	***Fig. 5b***	***Fig. 5c***	***Fig. 5d***
Casson								
Yield stress (τ_C), Pa	18.54 ± 0.26^{a}	15.71 ± 0.55^{b}	17.35 ± 0.28^{c}	12.11 ± 0.07^{d}	87.28 ± 2.02^{e}	74.75 ± 2.06^{f}	75.16 ± 1.33^{g}	48.61 ± 0.88^{h}
Plastic viscosity (η_C), Pa.s	1.90 ± 0.01^{a}	1.87 ± 0.03^{b}	1.94 ± 0.01^{c}	1.90 ± 0.01^{d}	8.42 ± 0.08^{e}	8.46 ± 0.14^{f}	8.19 ± 0.13^{g}	10.59 ± 0.11^{h}
Determination coefficient (R^2)	0.998	0.998	0.992	0.992	0.997	0.993	0.993	0.993
Windhab								
Static yield stress (τ_0), Pa	15.24 ± 0.14^{a}	12.35 ± 0.26^{b}	12.56 ± 0.10^{b}	9.99 ± 0.16^{c}	49.83 ± 5.32^{d}	69.56 ± 3.87^{e}	49.29 ± 2.71^{d}	42.72 ± 0.87^{f}
Dynamic yield stress (τ_1), Pa	25.01 ± 0.62^{a}	21.18 ± 1.55^{b}	32.07 ± 0.94^{c}	19.52 ± 0.57^{d}	102.19 ± 3.05^{e}	107.92 ± 7.89^{e}	120.75 ± 12.37^{e}	71.86 ± 1.36^{f}
Shear rate infinite viscosity ($\dot{\gamma}*$), s^{-1}	12.37 ± 1.58^{a}	11.18 ± 0.89^{a}	8.21 ± 1.08^{b}	6.03 ± 0.67^{b}	3.91 ± 0.46^{c}	9.30 ± 1.13^{d}	5.92 ± 1.90^{c}	2.10 ± 0.05^{e}
Infinite viscosity (η_∞), Pa.s	1.75 ± 0.01^{a}	1.73 ± 0.02^{b}	1.72 ± 0.02^{c}	1.79 ± 0.01^{d}	8.01 ± 0.10^{e}	7.40 ± 0.33^{f}	7.49 ± 0.03^{g}	8.79 ± 0.08^{h}
Determination coefficient (R^2)	0.999	0.999	0.999	0.999	0.999	0.996	0.999	0.999
Modified Herschel-Bulkley								
Yield stress (τ_0), Pa	14.30 ± 0.04^{a}	11.56 ± 0.18^{b}	9.26 ± 0.32^{c}	9.99 ± 0.12^{d}	62.60 ± 1.12^{e}	40.78 ± 2.46^{f}	47.51 ± 3.11^{g}	40.88 ± 0.76^{f}
Consistency index (k)	2.48 ± 0.12^{a}	2.45 ± 0.21^{b}	6.88 ± 0.60^{c}	2.71 ± 0.07^{d}	13.98 ± 0.98^{e}	19.96 ± 2.14^{e}	19.77 ± 1.96^{e}	16.24 ± 1.58^{e}
Power-law index (n)	0.82 ± 0.01^{a}	0.82 ± 0.01^{b}	0.47 ± 0.04^{c}	0.81 ± 0.00^{d}	0.81 ± 0.02^{e}	0.73 ± 0.02^{f}	0.55 ± 0.08^{g}	0.58 ± 0.10^{g}
Infinite viscosity (η_∞), Pa.s	0.73 ± 0.02^{a}	0.70 ± 0.02^{b}	1.33 ± 0.06^{c}	0.74 ± 0.01^{d}	2.20 ± 0.22^{e}	1.69 ± 0.64^{e}	5.60 ± 0.58^{f}	5.50 ± 1.67^{f}
Determination coefficient (R^2)	0.999	0.999	0.999	0.999	0.999	0.999	0.999	0.999

List of figures

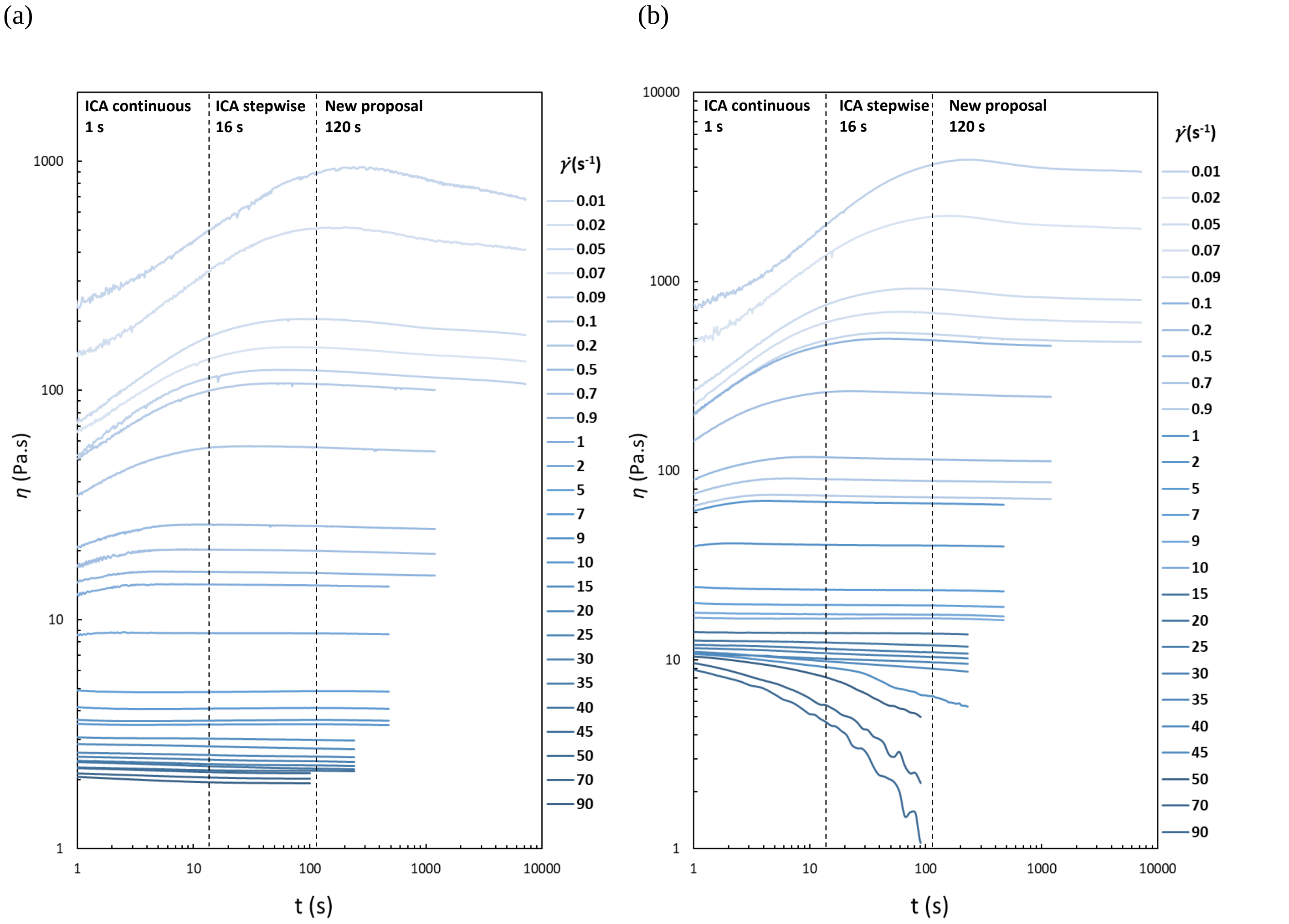

Fig. 1. Evolution of apparent viscosity of MV (left) and HV (right) as a function of time at corresponding shear rates measured with sandblasted parallel plate 50 mm.

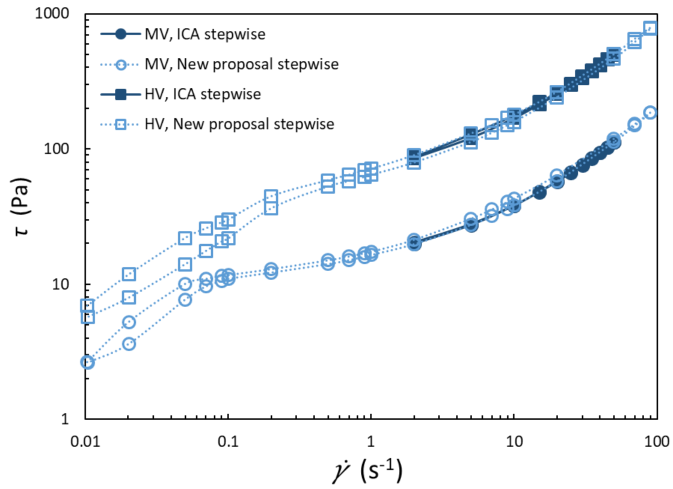

Fig. 2. Shear stress curve of MV (circle) and HV (square) measured with smooth concentric cylinder with two protocols: ICs (solid line) and NPs (dotted line).

(a) (b)

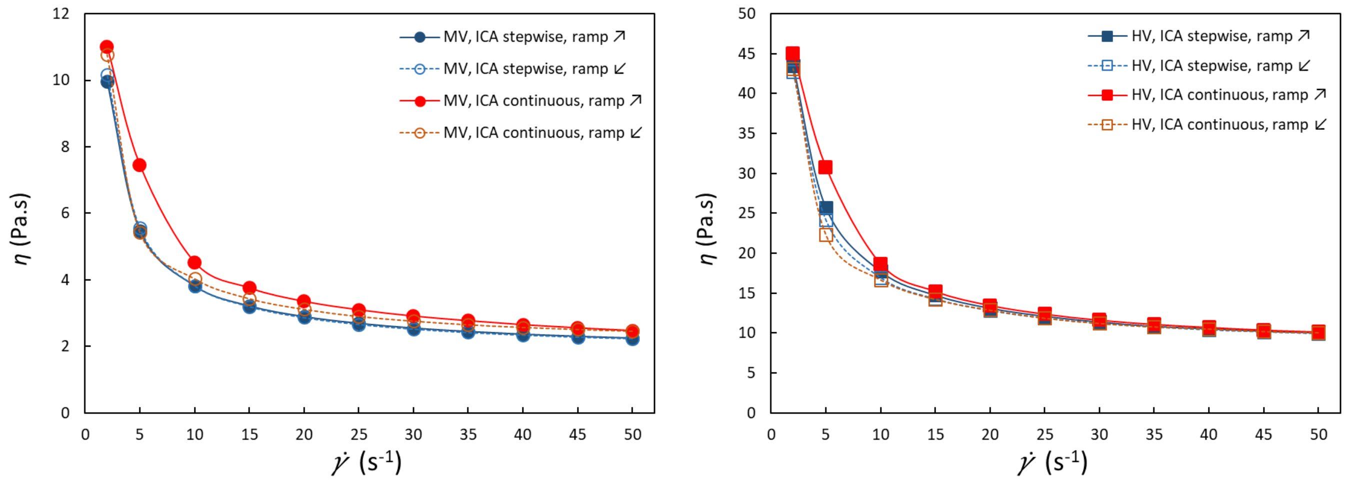

Fig. 3. Viscosity curve of MV (Fig. 2a) and HV (Fig. 2b) measured with concentric cylinder with two ICA protocols, stepwise (solid line) and continuous (dotted line).

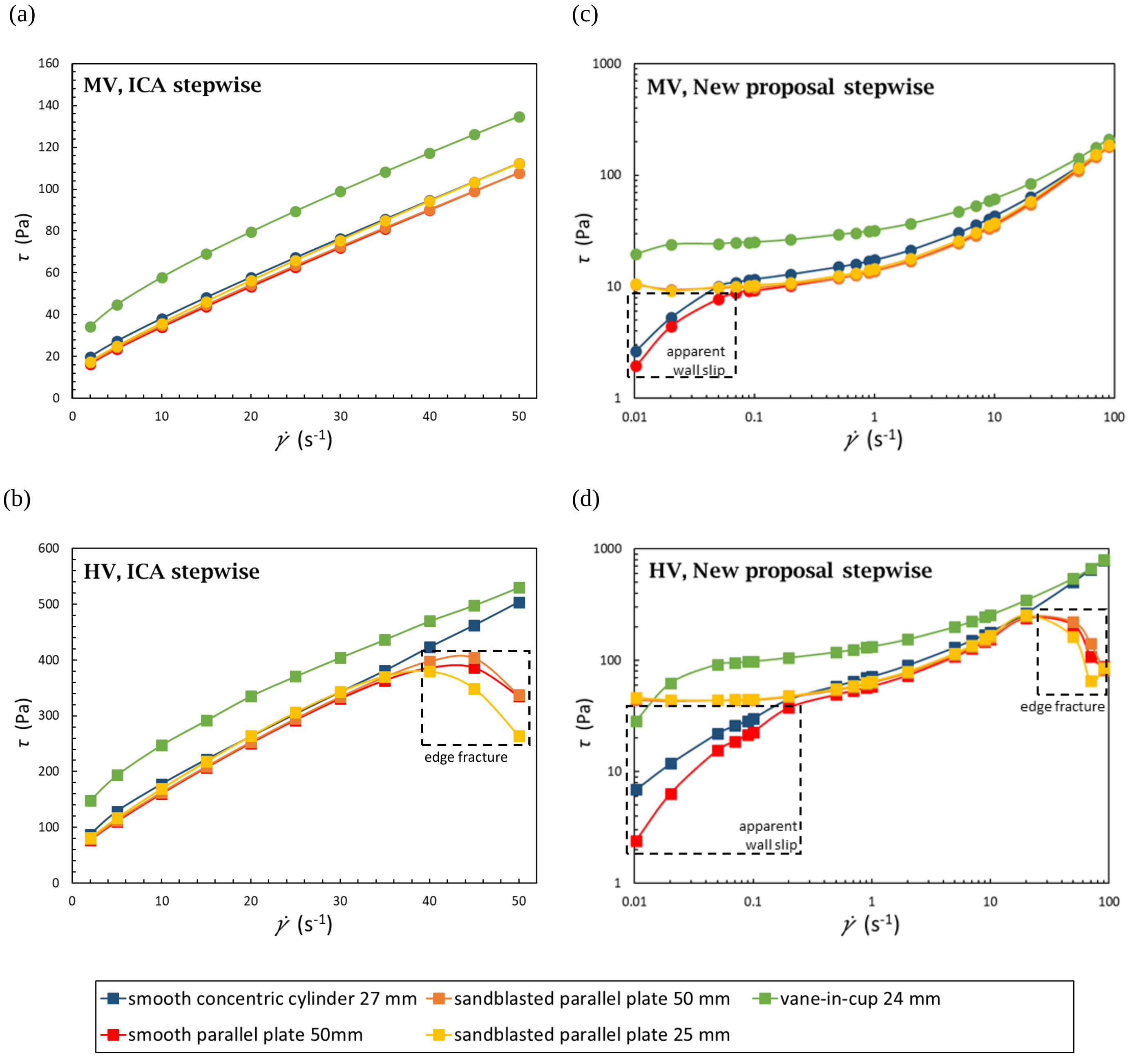

Fig. 4. Shear stress values of MV (circle) and HV (square) measured with smooth concentric cylinder (blue), smooth vane-in-cup (green), smooth parallel plate 50 mm (red), sandblasted parallel plate 50 mm (orange), sandblasted parallel plate 25 mm (yellow) in a flow curve. Left: ICA stepwise protocol. Right: New proposal stepwise protocol.

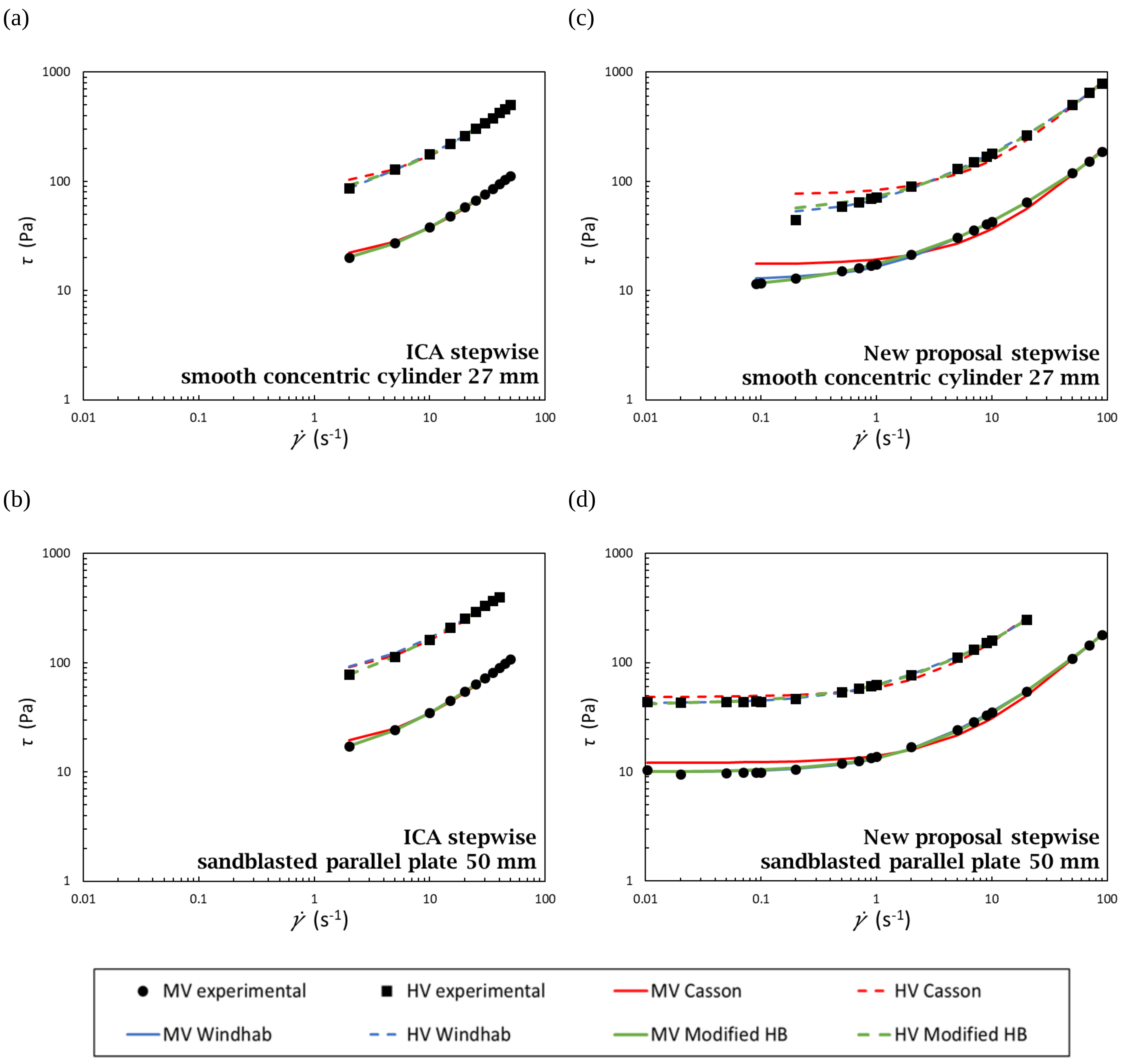

Fig. 5. Experimental shear stress values of MV (black circle) and HV (black square) in a flow curve and their corresponding data fittings of MV (solid line) and HV (striped line) using Casson (in red), Windhab (in blue) and modified Herschel-Bulkley (in green) mathematical model.

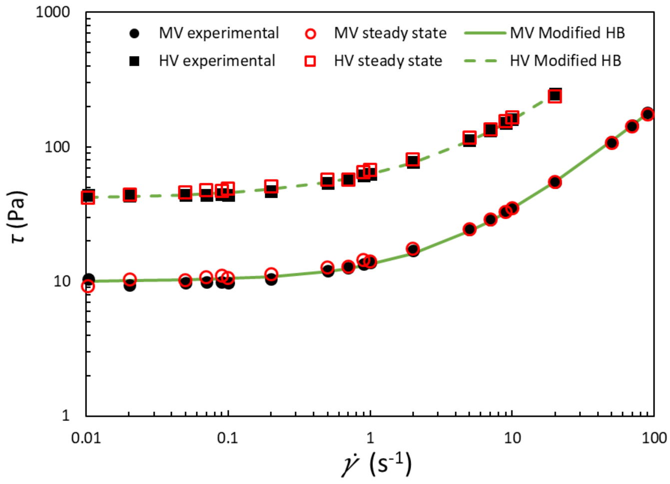

Fig. 6. Shear stress value of MV (solid black circle) and HV (solid black square) measured with new proposal stepwise protocol in comparison with steady-state shear stress at 120s of MV (empty red circle) and HV (empty red square) fitted with modified Herschel-Bulkley model (solid blue line for MV and striped blue line for HV). All measurement uses sandblasted parallel plate 50 mm.

Declarations

Ethics approval and consent to participate: Not applicable

Consent for publication: Not applicable

Competing interest: Not applicable

Author contributions: Nathaniel Hendrik: conceptualization, methodology, data collection, data analysis and interpretation, writing-original manuscript preparation and finalization. Flávio H. Marchesini: conceptualization, methodology, data interpretation, writing-reviewing and editing. Davy Van de Walle: conceptualization, methodology, data interpretation, writing-reviewing and editing. Koen Dewettinck: conceptualization, methodology and writing-reviewing.

Funding: This research was funded by the Special Research Fund (Bijzonder Onderzoeksfonds, BOF) of Ghent University, under the Concerted Research Actions Project (Geconcerteerde Onderzoeksacties, GoA) with project number BOF.GOA.2018.0002.03. We would like to thank Belcolade for providing the chocolates.

Availability of data and materials: The authors declare that the data supporting the findings of this study are available within the article.

References

Aeschlimann, J.M., & Beckett, S.T. (2000). International inter-laboratory trials to determine the factors affecting the measurement of chocolate viscosity. *Journal of Texture Studies* 31(5), 541-576. https://doi.org/10.1111/j.1745-4603.2000.tb01019.x.

Afoakwa, E.O., Paterson, A., & Fowler, M. (2008). Effects of particle size distribution and composition on rheological properties of dark chocolate. *European Food Research and Technology* 226(6), 1259-1268. https://doi.org/10.1007/s00217-007-0652-6.

Afoakwa, E.O., Paterson, A., Fowler, M., & Vieira, J. (2009). Comparison of rheological models for determining dark chocolate viscosity. *International Journal of Food Science & Technology* 44(1), 162-167. https://doi.org/10.1111/j.1365-2621.2008.01710.x.

AOAC, 1990a. Fat in Cacao Products. Soxhlet Extraction Method, Official Method 963.15, 15 ed. Association of Official Analytical Chemists International.

AOAC, 1990b. Loss on Drying (Moisture) in Cacao Products, Official Method 931.04, 15 ed. Association of Official Analytical Chemists International.

Baker, B.S., Brown, B.D., & Anantheswaran, R.C. (2006). Measurement of yield stress in dark chocolate using controlled stress vane method. *Journal of Texture Studies* 37(6), 655-667. https://doi.org/10.1111/j.1745-4603.2006.00076.x.

Baldino, N., Gabriele, D., & Migliori, M. (2010). The influence of formulation and cooling rate on the rheological properties of chocolate. *European Food Research and Technology* 231(6), 821-828. https://doi.org/10.1007/s00217-010-1334-3.

Barnes, H.A. (1995). A review of the slip (wall depletion) of polymer solutions, emulsions and particle suspensions in viscometers: its cause, character, and cure. *Journal of Non-Newtonian Fluid Mechanics* 56(3), 221-251. https://doi.org/10.1016/0377-0257(94)01282-M.

Barnes, H.A. (1997). Thixotropy—a review. *Journal of Non-Newtonian Fluid Mechanics* 70(1), 1-33. https://doi.org/10.1016/S0377-0257(97)00004-9.

Barnes, H.A. (2000). Measuring the viscosity of large-particle (and flocculated) suspensions - a note on the necessary gap size of rotational viscometers.

Barnes, H.A., Eastwood, A.R., & Yates, B. (1975). A comparison of the rheology of two polymeric and two micellar systems. Part II: Second normal stress difference. *Rheologica Acta* 14(1), 61-70. https://doi.org/10.1007/BF01527213.

Barnes, H.A., & Nguyen, Q.D. (2001). Rotating vane rheometry — a review. *Journal of Non-Newtonian Fluid Mechanics* 98(1), 1-14. https://doi.org/10.1016/S0377-0257(01)00095-7.

Bergemann, N., Heil, M., Smith, B., & Juel, A. (2018). From elastic deformation to flow in tempered chocolate. *Journal of Rheology* 62(5), 1187-1195. https://doi.org/10.1122/1.5038253.

Bolenz, S., & Tischer, T. (2013). Measuring shear stress at lowest possible shear rates and improving viscosity determination of fat suspensions, for example chocolates. *International Journal of Food Science & Technology*, n/a-n/a. https://doi.org/10.1111/ijfs.12232.

Buscall, R., McGowan, J.I., & Morton-Jones, A.J. (1993). The rheology of concentrated dispersions of weakly attracting colloidal particles with and without wall slip. *Journal of Rheology* 37(4), 621-641. https://doi.org/10.1122/1.550387.

Chevalley, J. (1994). Chocolate flow properties. In S.T. Beckett (Ed.), *Industrial Chocolate Manufacture and Use* (pp. 139-155). Springer US, Boston, MA. https://doi.org/ 10.1007/978-1-4615-2111-2_10.

Coussot, P. (2005). *Rheometry of Pastes, Suspensions, and Granular Materials: Applications in Industry and Environment* pp. 1-291). https://doi.org/10.1002/0471720577.

de Souza Mendes, P.R. (2011). Thixotropic elasto-viscoplastic model for structured fluids. *Soft Matter* 7(6), 2471-2483. https://doi.org/10.1039/c0sm01021a.

de Souza Mendes, P.R., Alicke, A.A., & Thompson, R.L. (2014). Parallel-Plate geometry correction for transient rheometric experiments. *APPLIED RHEOLOGY* 24(5), 1-10. https://doi.org/doi:10.3933/applrheol-24-52721.

Do, T.A.L., Hargreaves, J.M., Wolf, B., Hort, J., & Mitchell, J.R. (2007). Impact of particle size distribution on rheological and textural properties of chocolate models with reduced fat content. *Journal of Food Science* 72(9), E541-E552. https://doi.org/10.1111/j.1750-3841.2007.00572.x.

Dzuy, N.Q., & Boger, D.V. (1983). Yield Stress Measurement for Concentrated Suspensions. *Journal of Rheology* 27(4), 321-349. https://doi.org/10.1122/1.549709.

Fernandes, V.A., Müller, A.J., & Sandoval, A.J. (2013). Thermal, structural and rheological characteristics of dark chocolate with different compositions. *Journal of Food Engineering* 116(1), 97-108. https://doi.org/10.1016/j.jfoodeng.2012.12.002.

Fischer, P. (2015). Rheological properties of food. In L. Nollet, F. Toldra (Eds.), *Handbook of food analysis - Two volume set* (pp. 21-38). CRC Press, Boca Raton.

García, M.C., Alfaro, M.C., & Muñoz, J. (2015). Yield stress and onset of nonlinear time-dependent rheological behaviour of gellan fluid gels. *Journal of Food Engineering* 159, 42-47. https://doi.org/10.1016/j.jfoodeng.2015.02.024.

Glicerina, V., Balestra, F., Dalla Rosa, M., & Romani, S. (2015). Effect of manufacturing process on the microstructural and rheological properties of milk chocolate. *Journal of Food Engineering* 145, 45-50. https://doi.org/10.1016/j.jfoodeng.2014.06.039.

Glicerina, V., Balestra, F., Dalla Rosa, M., & Romani, S. (2016). Microstructural and rheological characteristics of dark, milk and white chocolate: A comparative study. *Journal of Food Engineering* 169, 165-171. https://doi.org/10.1016/j.jfoodeng.2015.08.011.

Gray, M.P. (2017). Moulding, enrobing and cooling chocolate products. In S. Beckett, M.S. Fowler, G.R. Ziegler (Eds.), *Beckett's industrial chocolate manufacture and use* (pp. 356-399). John Wiley & Sons Ltd, Chichester, West Sussex.

Green, H., & Weltmann, R.N. (1943). Analysis of the Thixotropy of Pigment-Vehicle Suspensions Basic Principles of the Hysteresis Loop. *Industrial and Engineering Chemistry - Analytical Edition* 15(3), 201-206. https://doi.org/10.1021/i560115a015.

Ianni, F., Di Leonardo, R., Gentilini, S., & Ruocco, G. (2008). Shear-banding phenomena and dynamical behavior in a Laponite suspension. *Physical Review E* 77(3), 031406. https://doi.org/10.1103/PhysRevE.77.031406.

ICA, 2000. Viscosity of cocoa and chocolate products., Analytical method 46. CAOBISCO, Bruxelles, Belgium.

Keentok, M., & Xue, S.C. (1999). Edge fracture in cone-plate and parallel plate flows. *Rheologica Acta* 38(4), 321-348. https://doi.org/10.1007/s003970050184.

Manneville, S. (2008). Recent experimental probes of shear banding. *Rheologica Acta* 47(3), 301-318. https://doi.org/10.1007/s00397-007-0246-z.

Mansard, V., & Colin, A. (2012). Local and non local rheology of concentrated particles. *Soft Matter* 8(15), 4025-4043. https://doi.org/10.1039/c2sm25306b.

Mantihal, S., Prakash, S., Godoi, F.C., & Bhandari, B. (2019). Effect of additives on thermal, rheological and tribological properties of 3D printed dark chocolate. *Food Research International* 119, 161-169. https://doi.org/10.1016/j.foodres.2019.01.056.

Marchesini, F.H., Naccache, M.F., Abdu, A., Alicke, A.A., & de Souza Mendes, P.R. (2015). Rheological characterization of yield-stress materials: Flow pattern and apparent wall slip. *APPLIED RHEOLOGY* 25(5). https://doi.org/10.3933/APPLRHEOL-25-53883.

Meeten, G., & Sherwood, J., 1992. Vane technique for shear-sensitive and wall-slipping fluids, in: P.K. Moldenaers, R (Ed.) 11th International Congress on Rheology. Elsevier, Amsterdam, pp. 935-937.

Mewis, J., & Wagner, N.J. (2009). Thixotropy. *Advances in Colloid and Interface Science* 147-148(C), 214-227. https://doi.org/10.1016/j.cis.2008.09.005.

Mezger, T.G. (2014). *The Rheology Handbook* (4th edition ed. Vincentz Network, Hanover, Germany.

NCA/CMA (1988). Application of the Casson Viscosity Method for Chocolate to the Brookfield Viscometer. *Manufacturing Confectioner* 68(1), 73.

Oba, S., Toker, O.S., Palabiyik, İ., Konar, N., Goktas, H., Cukur, Y., Artik, N., & Sagdic, O. (2017). Rheological and melting properties of sucrose-free dark chocolate. *International Journal of Food Properties,* 1-11. https://doi.org/10.1080/10942912.2017.1362652.

OICC (1973). Viscosity of chocolate - Determination of Casson yield value and Casson plastic viscosity. *Int. Choc. Review* 28(9), 223.

Ovarlez, G., Mahaut, F., Bertrand, F., & Chateau, X. (2011). Flows and heterogeneities with a vane tool: Magnetic resonance imaging measurements. *Journal of Rheology* 55(2), 197-223. https://doi.org/10.1122/1.3526349.

Rathee, V., Monti, A., Rosti, M.E., & Shen, A.Q. (2021). Shear thickening behavior in dense repulsive and attractive suspensions of hard spheres. *Soft Matter* 17(35), 8047-8058. https://doi.org/10.1039/d1sm00971k.

Rodrigues, S.A., Shewan, H.M., Xu, Y., Selway, N., & Stokes, J.R. (2021). Frictional behaviour of molten chocolate as a function of fat content. *Food & Function* 12(6), 2457-2467. https://doi.org/10.1039/D0FO03378B.

Rohm, H., Böhme, B., & Skorka, J. (2018). The impact of grinding intensity on particle properties and rheology of dark chocolate. *LWT - Food Science and Technology* 92, 564-568. https://doi.org/10.1016/j.lwt.2018.03.006.

Saputro, A.D., Van de Walle, D., Caiquo, B.A., Hinneh, M., Kluczykoff, M., & Dewettinck, K. (2019). Rheological behaviour and microstructural properties of dark chocolate produced by combination of a ball mill and a liquefier device as small scale chocolate production system. *LWT - Food Science and Technology* 100, 10-19. https://doi.org/10.1016/j.lwt.2018.10.039.

Schantz, B., & Rohm, H. (2005). Influence of lecithin–PGPR blends on the rheological properties of chocolate. *LWT - Food Science and Technology* 38(1), 41-45. https://doi.org/10.1016/j.lwt.2004.03.014.

Servais, C., Ranc, H., & Roberts, I.D. (2003). Determination of chocolate viscosity. *Journal of Texture Studies* 34(5-6), 467-497.

Sokmen, A., & Gunes, G. (2006). Influence of some bulk sweeteners on rheological properties of chocolate. *LWT - Food Science and Technology* 39(10), 1053-1058. https://doi.org/10.1016/j.lwt.2006.03.002.

Talansier, E., Bacconnier, A., Caton, F., Chastel, C., Costa, L., Gunes, D.Z., & Roux, D.C.D. (2019). Accurate methodology to determine slip velocity, yield stress and the constitutive relation for molten chocolate. *Journal of Food Engineering* 244, 220-227. https://doi.org/10.1016/j.jfoodeng.2018.09.031.

Taylor, J.E., Van Damme, I., Johns, M.L., Routh, A.F., & Wilson, D.I. (2009). Shear rheology of molten crumb chocolate. *Journal of Food Science* 74(2), E55-61. https://doi.org/10.1111/j.1750-3841.2008.01041.x.

van der Vaart, K., Depypere, F., Graef, V.D., Schall, P., Fall, A., Bonn, D., & Dewettinck, K. (2013). Dark chocolate’s compositional effects revealed by oscillatory rheology. *European Food Research and Technology* 236(6), 931-942. https://doi.org/10.1007/s00217-013-1949-2.

Vásquez, C., Henríquez, G., López, J.V., Penott-Chang, E.K., Sandoval, A.J., & Müller, A.J. (2019). The effect of composition on the rheological behavior of commercial chocolates. *LWT - Food Science and Technology* 111, 744-750. https://doi.org/10.1016/j.lwt.2019.05.101.

Wilson, L.L., Speers, R.A., & Tung, M.A. (1993). Yield stresses in molten chocolates. *Journal of Texture Studies* 24(3), 269-286.

Windhab, E.J. (1995). Rheology in food processing. In S.T. Beckett (Ed.), *Physico-chemical aspects of food processing* (pp. 80-116). Blackie Academic and Professional, Glasgow. https://doi.org/ 10.1002/9781444301588.ch10.

Windhab, E.J. (2006). What makes for smooth, creamy chocolate? *Physics today* 59(6), 82.

Wolf, B. (2017). Chocolate flow properties. In S. Beckett, M.S. Fowler, G.R. Ziegler (Eds.), *Beckett's industrial chocolate manufacture and use* (pp. 274-297). John Wiley & Sons Ltd, Chichester, West Sussex.

Yeow, Y.L., Ko, W.C., & Tang, P.P.P. (2000). Solving the inverse problem of Couette viscometry by Tikhonov regularization. *Journal of Rheology* 44(6), 1335-1351. https://doi.org/10.1122/1.1308520.

Yoshimura, A., & Prud Homme, R.K. (1988). Wall Slip Corrections for Couette and Parallel Disk Viscometers. *Journal of Rheology* 32(1), 53-67. https://doi.org/10.1122/1.549963.